ARTHRITIS & RHEUMATOLOGY
Vol. 66, No. 8, August 2014, pp 2246–2258
DOI 10.1002/art.38679

Identification of Stage-Specific Genes Associated With Lupus Nephritis and Response to Remission Induction in (NZB × NZW)F1 and NZM2410 Mice

Ramalingam Bethunaickan,[1] Celine C. Berthier,[2] Weijia Zhang,[3] Ridvan Eksi,[2] Hong-Dong Li,[2] Yuanfang Guan,[2] Matthias Kretzler,[2] and Anne Davidson[1]

Objective. **To elucidate the molecular mechanisms involved in renal inflammation during the progression, remission, and relapse of nephritis in murine lupus models using transcriptome analysis.**

Methods. **Kidneys from (NZB × NZW)F1 (NZB/NZW) and NZM2410 mice were harvested at intervals during the disease course or after remission induction. Genome-wide expression profiles were obtained from microarray analysis of perfused kidneys. Real-time polymerase chain reaction (PCR) analysis for selected genes was used to validate the microarray data. Comparisons between groups using SAM, and unbiased analysis of the entire data set using singular value decomposition and self-organizing maps were performed.**

Results. **Few changes in the renal molecular profile were detected in prenephritic kidneys, but a significant shift in gene expression, reflecting inflammatory cell infiltration and complement activation, occurred at proteinuria onset. Subsequent changes in gene expression predominantly affected mitochondrial dysfunction and metabolic stress pathways. Endothelial cell activation, tissue remodeling, and tubular damage were the major pathways associated with loss of renal function. Remission induction reversed most, but not all, of the inflammatory changes, and progression toward relapse was associated with recurrence of inflammation, mitochondrial dysfunction, and metabolic stress signatures.**

Conclusion. **Immune cell infiltration and activation is associated with proteinuria onset and is reversed by immunosuppressive therapy, but disease progression is associated with renal hypoxia and metabolic stress. Optimal therapy for lupus nephritis may therefore need to target both immune and nonimmune disease mechanisms. In addition, the overlap of a substantial subset of molecular markers with those expressed in the kidneys of lupus patients suggests potential new biomarkers and therapeutic targets.**

Lupus nephritis affects 30–70% of patients with systemic lupus erythematosus (SLE), and its treatment remains insufficiently effective and excessively toxic (1–4). Although biomarkers for nephritis are being identified (5,6), there is still no reliable way of predicting an impending renal flare or determining which patients will respond to therapy. Because human renal tissue cannot be obtained sequentially during remission and relapse, animal models are often used to study the progression of lupus nephritis.

Complete histologic remission of proliferative glomerulonephritis is induced in 80–90% of (NZB × NZW)F1 (NZB/NZW) mice (7,8) by a combination of cyclophosphamide (CYC) and the costimulatory antagonists CTLA-4Ig and anti-CD40L (triple therapy) (9), or a combination of CTLA-4Ig with a BAFF antagonist (ref. 10 and Davidson A: unpublished observations). Similarly, BAFF-R-Ig induces long-lasting remission of

Supported by the NIH (National Institute of Diabetes and Digestive and Kidney Diseases grant R01-DK-085241-01).

[1]Ramalingam Bethunaickan, PhD, Anne Davidson, MBBS: Feinstein Institute for Medical Research, Manhasset, New York; [2]Celine C. Berthier, PhD, Ridvan Eksi, MSc, Hong-Dong Li, PhD, Yuanfang Guan, PhD, Matthias Kretzler, MD: University of Michigan, Ann Arbor; [3]Weijia Zhang, PhD: Mount Sinai Medical Center, New York, New York.

Drs. Bethunaickan and Berthier contributed equally to this work.

Address correspondence to Anne Davidson, MBBS, Center for Autoimmunity and Musculoskeletal Diseases, Feinstein Institute for Medical Research, 350 Community Drive, Manhasset, NY 11030. E-mail: adavidson1@nshs.edu.

Submitted for publication November 1, 2013; accepted in revised form April 17, 2014.

nephritis in NZM2410 mice that ordinarily develop glomerulosclerosis with rapid progression to renal failure (11). The induced remission does not abrogate renal immune complex deposition but is associated with decreased renal inflammation and preservation of the glomerular filtration barrier (11,12). Evidence from multiple murine models confirms that there is a checkpoint in disease progression between immune complex deposition and the development of renal impairment (13–15).

In this study, we profiled NZB/NZW mouse kidneys to define the molecular characteristics of nephritis onset and progression, complete remission, and progression toward relapse. Surprisingly, only a few changes in the renal gene expression profile were detected after immune complex deposition, but a major shift in transcripts occurred at proteinuria onset, reflecting the rapid onset of inflammation. Subsequent changes in gene expression reflected mitochondrial dysfunction and metabolic stress. Remission induction reversed much of the inflammatory gene expression pattern, but during late remission mitochondrial dysfunction and metabolic stress signatures recurred before proteinuria onset. In NZM2410 mice, a limited inflammatory signature arose during remission but was not associated with renal decline. In both strains, the presence of proteinuria was closely associated with renal tubular dysfunction. Our findings suggest that optimal therapy for SLE nephritis may need to target both immune and nonimmune disease mechanisms.

MATERIALS AND METHODS

Mouse models and treatment protocols. Female NZB/NZW mice (The Jackson Laboratory) were followed up clinically as previously described (9,16,17). Mice with proteinuria of >300 mg/dl on 2 occasions 24–48 hours apart were treated with a single dose of 50 mg/kg of CYC and 6 doses of 100 μg of CTLA-4Ig and 250 μg of anti-CD40L (CD154) (9). Remission was defined as proteinuria of ≤30 mg/dl on ≥2 occasions. An early remission group was killed 3–4 weeks after remission induction and had complete histologic remission by light microscopy, as defined by composite glomerular and tubulointerstitial scores of ≤2.5, similar to young controls. The late remission group was killed >5–14 weeks after remission induction and had composite glomerular and tubulointerstitial scores of ≥3.0 (see Supplementary Figure 1, available on the *Arthritis & Rheumatology* web site at http://onlinelibrary.wiley.com/doi/10.1002/art.38679/abstract) (12). We also induced remission in 30-week-old mice with proteinuria of 100–300 mg/dl using a single dose of adenovirus expressing TACI-Ig, together with 2 weeks of CTLA-4Ig (100 μg 3 times per week) (10). These mice were killed 15 weeks after remission induction therapy; their renal scores were similar to those of mice with disease in late remission.

Twenty-two–week-old NZM2410 mice (Taconic) were treated with adenovirus expressing BAFF-R-Ig and killed at 30–35 weeks or at 55 weeks of age as previously described (11).

Control mice were killed at sequential disease stages as previously described (16,17). The ages and mean renal scores of each group are shown in Supplementary Table 1 (available on the *Arthritis & Rheumatology* web site at http://onlinelibrary.wiley.com/doi/10.1002/art.38679/abstract).

Analysis of renal tissues. Hematoxylin and eosin–stained kidney sections were scored for glomerular and interstitial damage using a semiquantitative scale of 0–4 (18). Renal RNA extraction, complementary DNA (cDNA) synthesis, hybridization, microarray processing, data normalization, and filtering were performed as previously described (16,17). Significantly regulated genes were analyzed using Genomatix Pathway System (GePS; www.genomatix.de) and Ingenuity Pathway Analysis (IPA; www.ingenuity.com) software. Gene expression data sets are available at GEO accession nos. GSE49898, GSE32583, and GSE32591.

Identification of coherent expression modules using self-organizing map (SOM) analysis. To identify the biologic processes driving coherent expression modules, we used SOM analysis to extract the fundamental patterns of gene expression inherent in the serial data sets from NZB/NZW mice (19). The average expression values across multiple samples were taken for each gene for each disease stage. To capture the dynamic trend across different stages, we centered the expression pattern for each gene across all stages at 0 and then applied SOM analysis to identify the coherent expression modules (19). We used IPA software to identify significantly represented biologic processes.

Identification of major expression patterns using singular value decomposition (SVD). To detect major expression responses during disease progression, we applied SVD on the time course data. SVD is a mainstream technique for analysis of multivariate time course data to identify orthogonal patterns. It allows us to transform genome-wide expression data from genes × arrays space to diagonalized "eigengenes" × "eigenassays" space (20). The eigengenes (also referred to as patterns) represent orthogonal expression patterns that may be hidden in the original data (20–22). The top 600 genes in the dominant pattern for each comparison were further analyzed.

Real-time quantitative polymerase chain reaction (qPCR). Real-time qPCR analysis of 166 genes was performed as previously described (12,16,23).

Statistical analysis. The Institute for Genomic Research MultiExperiment Viewer application was used for statistical analysis of microarray data as previously described (16,17). Genes undergoing further analyses met the following criteria: q value ≤0.05 and absolute value of $\log_2$ fold change ≥0.26. Genes that met the above criteria and whose mean fold expression changed by ≥1.5 fold between the nephritic and remission stages were considered to be reversed with remission. The qPCR data were scaled to the mean of the young mice in each strain, given a value of 1. Genes with q value (false discovery rate) of <0.05 were considered significant (16,17). Since all pathways in the GePS are derived from *Homo sapiens*,

Table 1. Top significantly regulated canonical pathways and molecules in each pathway in mice with new-onset proteinuria versus mice without proteinuria and in mice with established proteinuria versus mice with new-onset proteinuria, as assessed by IPA*

Pathway	*P*	No. of genes regulated	No of genes in pathway	Genes
Top pathways of genes regulated in mice with new-onset proteinuria versus mice without proteinuria†				
Dendritic cell maturation	4.37×10^{-9}	35	207	B2M, ICAM1, NFKBIE, HLA–DQA1, LTB, HLA–DRB1, CD83, HLA–DMB, HLA–DQB1, FCGR1A, EP300, COL1A2, PLCE1, PIK3CG, HLA–B, COL18A1, STAT1, PLCD4, FCGR3A, HLA–DMA, TYROBP, FCGR2A, RELB, IKBKE, DDR1, TLR2, IL33, COL1A1, TLR4, IL18, FCER1G, CD86, IL1B, IRF8, COL3A1
Altered T cell and B cell signaling in RA	3.89×10^{-7}	21	92	TLR1, HLA–DMA, SPP1, CD79B, RELB, HLA–DQA1, HLA–DRB1, LTB, HLA–DMB, HLA–DQB1, TNFRSF17, IL33, TLR2, TLR4, IL18, CXCL13, TGFB1, FCER1G, CD86, IL1B, TNFSF13B
Antigen presentation pathway	3.63×10^{-6}	11	40	B2M, PSMB9, HLA–DMA, HLA–DQA1, HLA–B, HLA–DRB1, HLA–DMB, PSMB8, CD74, TAP1, TAP2
Atherosclerosis signaling	7.08×10^{-6}	24	136	APOE, VCAM1, ICAM1, CXCR4, PLA2G7, F3, TNFRSF12A, SELPG, COL1A2, IL33, PLA2G4A, COL1A1, ITGB2, IL18, CCL2, APOC3, TGFB1, IL1B, SERPINA1, S100A8, COL18A1, CCR2, ITGA4, COL3A1
TREM-1 signaling	1.0×10^{-5}	15	71	ITGB1, TLR1, ICAM1, TYROBP, CD83, STAT3, TLR2, TLR4, CXCL3, IL18, CCL2, CASP1, CD86, IL1B, ITGAX
Fcγ receptor–mediated phagocytosis in macrophages and monocytes	1.10×10^{-5}	21	102	FYN, ARPC1B, FCGR2A, ACTB, ACTA2, ARPC5, FCGR1A, PRKCZ, PLD4, HMOX1, ARF6, NCF1, ACTR3, PIK3CG, ARPC2, HCK, VAMP3, LYN, ARPC3, FCGR3A, PRKCB
Communication between innate and adaptive immune cells	1.10×10^{-5}	17	109	B2M, TLR1, HLA–DRB1, CD83, CCL5, TNFRSF17, IL33, CXCL10, TLR2, TLR4, IL18, FCER1G, HLA–B, CD86, CCL3L1/CCL3L3, IL1B, TNFSF13B
Complement system	1.23×10^{-5}	10	35	C1R, SERPING1, C3, C1S, CFI, C1QC, C1QA, C1QB, CFH, C3AR1
CD28 signaling in T helper cells	1.4×10^{-5}	23	132	HLA–DMA, FYN, PTPN6, ARPC1B, NFATC3, NFKBIE, MAP3K1, ARPC5, HLA–DQA1, HLA–DRB1, PTPRC, CD3G, FOS, JUN, ACTR3, PIK3CG, ARPC2, FCER1G, CD86, ARPC3
Cell cycle control of chromosomal replication	1.86×10^{-5}	10	31	MCM5, MCM3, MCM6, MCM2, CDT1, ORC6, CHECK2, MCM4, DBF4, MCM7
Top pathways of genes regulated in mice with established proteinuria versus mice with new-onset of proteinuria‡				
TCA cycle II (eukaryotic)	1.48×10^{-10}	9	41	SUCLA2, CS, SUCLG1, SDHD, IDH3A, MDH1, MDH2, ACO1, IDH3B
Mitochondrial dysfunction	4.90×10^{-6}	13	186	COX6B1, NDUFA9, COX6A1, COX11, SOD2, ATP5B, COX5A, NDUFB6, SDHD, CYC1, ATP5G3, NDUFA8, COX15
Inosine-5′-phosphate biosynthesis II	1.26×10^{-3}	2	16	ADSL, PAICS
Arsenate detoxification I (glutaredoxin)	2.51×10^{-3}	2	20	AS3MT, GSTO1
Aspartate degradation II	8.32×10^{-3}	2	14	MDH1, MDH2

* IPA = Ingenuity Pathway Analysis; RA = rheumatoid arthritis; TREM-1 = triggering receptor expressed on myeloid cells; TCA = tricarboxylic acid.

† Top 10 pathways of the 1,342 genes that were regulated in 23-week-old mice with new-onset proteinuria versus 23-week-old mice without proteinuria (corresponding to 1,194 human gene IDs).

‡ Top 5 pathways of the 321 genes that were regulated in 36-week-old mice with established proteinuria versus 23-week-old mice with new-onset proteinuria (corresponding to 311 human gene IDs).

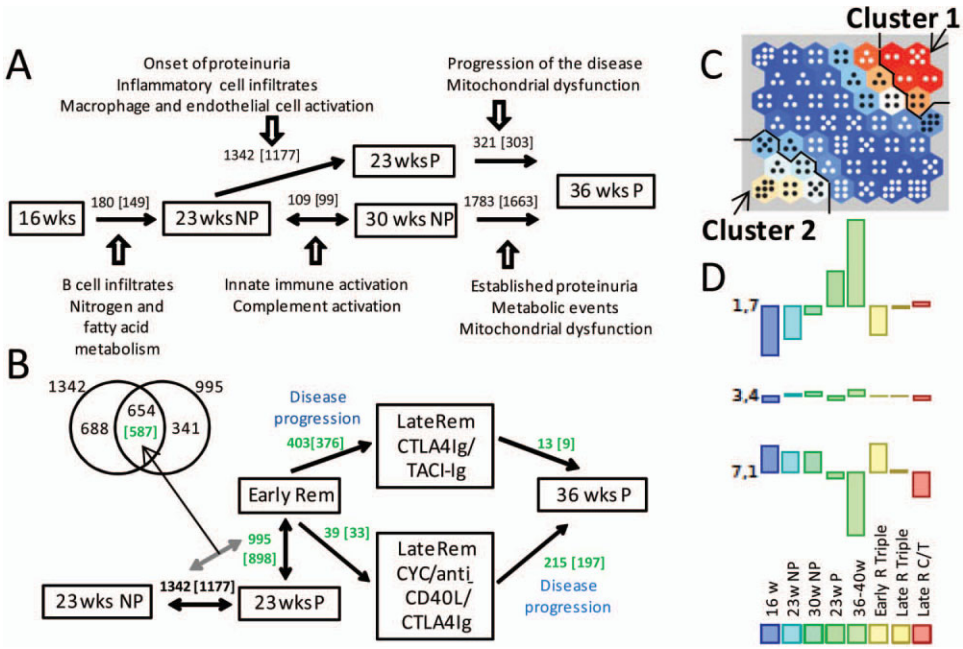

Figure 1. Patterns of gene expression in (NZB × NZW)F1 (NZB/NZW) mice. **A,** Diagram showing the numbers of genes regulated between the indicated stages of disease progression. Dominant pathologic processes identified by Ingenuity Pathway Analysis are shown for each disease stage. Numbers shown in brackets are the number of human orthologs. **B,** Diagram showing the numbers of genes regulated between the indicated stages before (black) and after (green) remission induction. The Venn diagram shows that 654 genes were regulated both during proteinuria onset and remission. **C,** Self-organizing map of data sets from each of the disease stages shown in **D**. The number of dots in each module reflects the number of genes regulated, and the color reflects the degree of change, either up (orange to red, with red reflecting the most change [cluster 1]) or down (white to beige, with beige reflecting the most change [cluster 2]) or unchanged (blue). **D,** Average gene expression for each data set in 3 representative modules (modules 1,7; 3,4; and 7,1). Data sets were from 16-week-old mice, 23-week-old mice without proteinuria (23w NP), 30-week-old mice without proteinuria, 23-week-old mice with proteinuria (23w P), 36–40-week-old mice; mice with disease in early remission treated with triple therapy (cyclophosphamide [CYC], CTLA-4Ig, and anti-CD40L; early R triple), mice with disease in late remission treated with triple therapy, and mice with disease in late remission treated with CTLA-4Ig and TACI-Ig (Late R C/T).

the mouse gene IDs were converted to the corresponding human orthologs using the NCBI homolog (build 67) for all GePS and IPA analyses.

The comparisons shown in Supplementary Table 1 (available on the *Arthritis & Rheumatology* web site at http://onlinelibrary.wiley.com/doi/10.1002/art.38679/abstract) were performed using Mann-Whitney test. *P* values less than or equal to 0.05 were considered significant.

RESULTS

Gene expression profile associated with disease onset. Only 180 changes in gene expression were found between 16-week-old mice and 23-week-old mice without proteinuria. The major signature was for immunoglobulin genes and B cells (see Supplementary Table 2A, available on the *Arthritis & Rheumatology* web site at http://onlinelibrary.wiley.com/doi/10.1002/art.38679/abstract). Indeed, small lymphoid aggregates containing plasma cells are found in the renal pelvis of 23-week-old old NZB/NZW mice (results not shown). Other pathways included nitrogen metabolism and fatty acid synthesis.

Similarly, only 109 genes were regulated between 23-week-old mice and 30-week-old mice without proteinuria, reflecting innate immune cell activation, complement protein production, early tubular involvement, and collagen gene expression (see Supplementary Table 2B, available on the *Arthritis & Rheumatology* web site at http://onlinelibrary.wiley.com/doi/10.1002/art.38679/abstract). In contrast, major shifts in gene expression were observed when 23-week-old mice without proteinuria were compared with 23-week-old mice with new-onset proteinuria (1,342 genes regulated) (see Supplementary Table 2C). IPA indicated that immune activation accounted for the top 10 pathways (Table 1).

Table 2. Top significantly regulated canonical pathways and molecules in each pathway for the 654 genes that were up-regulated in mice at onset of proteinuria and reversed upon remission, as assessed by IPA*

Pathway	*P*	No. of genes regulated	No of genes in pathway	Genes
Dendritic cell maturation	6.31×10^{-8}	22	185	B2M, ICAM1, TYROBP, FCG2RA, RELB, NFKBIE, HLA–DQA1, IKBKE, CD83, FCGR1A, COL1A2, IL33, TLR2, TLR4, IL18, PIK3CG, HLA–DRA, CD86, IL1B, IRF8, STAT1, HLA–C
Communication between innate and adaptive immune cells	1.38×10^{-7}	15	109	B2M, CD83, CCL5, CCL9, IL33, CXCL10, TLR2, TLR4, IL18, HLA–DRA, IL1B, TLR13, CD86, TNFSF13B, HLA–C
Cell cycle control of chromosomal replication	9.77×10^{-7}	9	31	MCM5, MCM3, MCM6, MCM2, CDT1, ORC6, MCM4, DBF4, MCM7
TREM-1 signaling	6.03×10^{-6}	11	66	TLR2, TLR4, IL18, ICAM1, CCL2, TYROBP, CASP1, TLR3, CD86, IL1B, CD83
Hepatic fibrosis/hepatic stellate cell activation	2.29×10^{-5}	18	147	CCR5, VCAM1, ICAM1, FN1, CTGF, MMP2, CCL5, COL1A2, MYL9, CXCL3, TLR4, LY96, CCL2, IL10RA, CD14, IL1B, STAT1, PDGFRB
MSP-Ron signaling pathway	7.41×10^{-5}	9	51	TLR2, CSF2RB, ITGB2, TLR4, KLK3, CCL2, PIK3CG, ACTB, CCR2
Complement system	7.76×10^{-5}	7	35	C1R, SERPING1, C3, C1S, C1QA, C1QB, CFH
Altered T cell and B cell signaling in RA	1.17×10^{-4}	12	92	IL33, TLR2, TLR4, IL18, SPP1, RELB, HLA–DRA, HLA–DQA1, TLR13, CD86, IL1B, TNFSF13B
Role of hypercytokinemia/ hyperchemokinemia in the pathogenesis of influenza	1.32×10^{-4}	7	44	IL33, CXCL10, IL18, CCR5, CCL2, IL1B, CCL5
Role of pattern recognition receptors in recognition of bacteria and viruses	1.58×10^{-4}	13	106	C3, C1QA, C1QB, CCL5, TLR2, IFIH1, TLR4, CLEC7A, IRF7, PI3CG, CASP1, IL1B, CLEC6A

* The top 10 pathways of the 654 genes that were up-regulated in mice at onset of proteinuria and reversed upon remission (corresponding to 587 human gene IDs) are shown. MSP = macrophage-signaling pathway (see Table 1 for definitions).

Tubular damage was exemplified by increased expression of LCN2, FN1, and VIM. Further up-regulation of several collagen genes indicated early interstitial fibrosis.

Gene expression profile associated with disease progression. There were 321 gene differences between the kidneys of 23-week-old old mice with new-onset proteinuria and those of older mice with established proteinuria of >2 weeks' duration; these, surprisingly, were all down-regulated (see Supplementary Table 2D, available on the *Arthritis & Rheumatology* web site at http://onlinelibrary.wiley.com/doi/10.1002/art.38679/abstract). IPA indicated that the top 5 pathways involved metabolic alterations and mitochondrial dysfunction (Table 1).

Major changes in gene expression were observed between 30-week-old mice without proteinuria and 36-week-old mice with established proteinuria (see Supplementary Table 2E, available on the *Arthritis & Rheumatology* web site at http://onlinelibrary.wiley.com/doi/10.1002/art.38679/abstract). The 427 up-regulated genes reflected inflammation, similar to the pattern observed at disease onset (see Supplementary Table 3A, available on the *Arthritis & Rheumatology* web site at http://onlinelibrary.wiley.com/doi/10.1002/art.38679/abstract). The 1,356 down-regulated genes reflected metabolic and mitochondrial dysfunction, as observed during the progression of nephritis from onset to established disease (see Supplementary Table 3B). Gene expression changes during disease onset and progression are summarized in Figure 1A.

Transcriptional indicators of disease remission. To identify mechanisms of remission and transcriptional indicators of renal clinical status, we identified genes whose expression changed at proteinuria onset and reversed upon remission. Of the 1,342 genes that were up-regulated at proteinuria onset, 654 (48.7%) reversed, 603 by >1.5 fold, during complete remission (Figure 1B). (Also see Supplementary Table 2F, available on the *Arthritis & Rheumatology* web site at http://onlinelibrary.wiley.com/doi/10.1002/art.38679/abstract.) These genes reflected inflammatory cell infiltration, complement activity, endothelial cell activation, and extracellular matrix formation (Table 2 and Supplementary Figure 2A, available on the *Arthritis & Rheumatology* web site at http://onlinelibrary.wiley.com/doi/10.1002/art.38679/abstract). To determine the relevance to human disease, we interrogated data sets of genes up-regulated in the glomeruli and tubulointerstitium of SLE nephritis bi-

Table 3. Top 5 canonical pathways significantly regulated for the genes in each module of the SOM analysis, as assessed by IPA*

Module	Pathway	*P*
Cluster 1 (915 genes)		
1_6	IL-12 signaling and production in macrophages	1.58×10^{-6}
1_6	Prolactin signaling	7.59×10^{-5}
1_6	PKCθ signaling in T lymphocytes	8.32×10^{-5}
1_6	CTLA-4 signaling in cytotoxic T lymphocytes	1.17×10^{-4}
1_6	Granulocyte adhesion and diapedesis	9.33×10^{-5}
1_7	Granulocyte adhesion and diapedesis	1.58×10^{-12}
1_7	Altered T cell and B cell signaling in RA	1.26×10^{-13}
1_7	Dendritic cell maturation	2.00×10^{-13}
1_7	Agranulocyte adhesion and diapedesis	3.09×10^{-10}
1_7	Communication between innate and adaptive immune cells	4.90×10^{-10}
2_6	Semaphorin signaling in neurons	7.59×10^{-6}
2_6	Toll-like receptor signaling	8.51×10^{-6}
2_6	Tec kinase signaling	8.91×10^{-6}
2_6	LXR/RXR activation	6.76×10^{-5}
2_6	CD28 signaling in T helper cells	6.76×10^{-5}
2_7	Cell cycle control of chromosomal replication	5.37×10^{-5}
2_7	Role of IL-17A in psoriasis	2.29×10^{-3}
2_7	Estrogen-mediated S-phase entry	1.62×10^{-2}
2_7	p53 signaling	3.39×10^{-2}
2_7	Adenine and adenosine salvage III	3.98×10^{-2}
3_7	Mitotic roles of polo-like kinase	2.24×10^{-4}
3_7	$G_{\beta\gamma}$ signaling	1.41×10^{-3}
3_7	Chemokine signaling	2.34×10^{-3}
3_7	HGF signaling	2.51×10^{-3}
3_7	fMLP signaling in neutrophils	3.39×10^{-3}
Cluster 2 (1,728 genes)		
5_1	Catecholamine biosynthesis	2.88×10^{-5}
5_1	Mineralocorticoid biosynthesis	1.26×10^{-2}
5_1	Noradrenaline and adrenaline degradation	1.51×10^{-2}
5_1	Glucocorticoid biosynthesis	1.55×10^{-2}
5_1	VDR/RXR activation	1.55×10^{-2}
6_1	Flavin biosynthesis IV (mammalian)	1.58×10^{-4}
6_1	Tryptophan degradation X (mammalian, via tryptamine)	9.55×10^{-4}
6_1	Glutathione-mediated detoxification	2.88×10^{-3}
6_1	Glycogen degradation II	4.17×10^{-3}
6_1	Ethanol degradation II	4.07×10^{-3}
7_1	Ethanol degradation II	3.98×10^{-7}
6_2	Heme biosynthesis II	2.34×10^{-4}
6_2	Tetrapyrrole biosynthesis II	2.04×10^{-3}
6_2	Sphingomyelin metabolism	4.17×10^{-3}
6_2	Ubiquinol-10 biosynthesis (eukaryotic)	1.05×10^{-2}
6_2	Mitochondrial dysfunction	1.38×10^{-2}
7_2	Mitochondrial dysfunction	1.26×10^{-13}
7_3	Mitochondrial dysfunction	5.01×10^{-15}
7_1	Glycine betaine degradation	9.77×10^{-8}
7_1	Nicotine degradation II	3.24×10^{-7}
7_1	Superpathway of methionine degradation	1.35×10^{-6}
7_1	Serotonin degradation	1.74×10^{-6}
7_2	TCA cycle II (eukaryotic)	1.48×10^{-8}
7_2	Valine degradation I	1.26×10^{-4}
7_2	Branched-chain α-keto acid dehydrogenase complex	1.32×10^{-3}
7_2	Fatty acid β-oxidation I	8.51×10^{-4}
7_3	Fatty acid β-oxidation I	1.86×10^{-3}
7_3	L-glutamine biosynthesis II (tRNA-dependent)	3.39×10^{-4}
7_3	Coenzyme A biosynthesis	1.00×10^{-3}
7_3	Stearate biosynthesis I (animals)	3.02×10^{-3}

* SOM = self-organizing map; IPA = Ingenuity Pathway Analysis; IL-12 = interleukin-12; PKCθ = protein kinase Cθ; RA = rheumatoid arthritis; LXR = liver X receptor; RXR = retinoid X receptor; HGF = hepatocyte growth factor; VDR = vitamin D receptor; TCA = tricarboxylic acid; tRNA = transfer RNA.

opsy specimens compared with normal control biopsy specimens (17). A striking level of concordance was observed. Of the 654 mouse marker genes (corresponding to 587 human genes), 175 were concordantly regulated in both glomeruli and tubules of SLE nephritis biopsy specimens (see Supplementary Table 4A, available on the *Arthritis & Rheumatology* web site at http://onlinelibrary.wiley.com/doi/10.1002/art.38679/abstract), and a further 145 were concordantly regulated in one of the two compartments (Supplementary Table 4B). GePS analysis of the 175 shared genes revealed several nodes of pathogenic significance (Supplementary Figure 2B), including CD14 and CD18 (mononuclear cell infiltration/activation), CD44 (cell migration), Fn1 (extracellular matrix and fibrosis), CXCL10, CCL5, IL18 (chemokines/cytokines), and Stat1 (type I interferon [IFN] pathway). Stat1 was the most represented transcription factor; 54 of the 175 genes had a Stat1 binding site in their promoter (Supplementary Table 4C). Ig transcripts, CXCL13, and ITGAM were not completely down-regulated during remission, consistent with the persistence of small inflammatory infiltrates.

Gene expression profile associated with progression toward relapse. Only 39 differences were observed between early and late remission after triple therapy (see Supplementary Table 2G, available on the *Arthritis & Rheumatology* web site at http://onlinelibrary.wiley.com/doi/10.1002/art.38679/abstract). In contrast, 403 gene differences were noted between early remission and late remission after CTLA4-Ig/TACI-Ig treatment, and all were down-regulated and involved metabolic pathways (Supplementary Table 2H). Compared with mice studied late after triple therapy, mice with established proteinuria had 174 up-regulated genes and 41 down-regulated genes (Supplementary Table 2I). Only a few differences were observed between mice with established proteinuria and CTLA4-Ig/TACI-Ig–treated mice, confirming that these mice represent a later stage in the progressive relapse process. Gene expression changes during nephritis and early and late remission are summarized in Figure 1B.

Confirmation using SOM analysis. To identify genes that changed coherently throughout disease progression and remission, we applied SOM analysis, an unbiased approach to clustering genes based on the similarity between their sequential expression profiles. Figure 1C displays the SOM for this study. In the SOM panel, the top right set of modules (cluster 1, containing modules 1,6/1,7/2,6/2,7/3,7) includes mostly proinflammatory genes with coherent expression throughout the study. In contrast, the bottom left set of modules (cluster 2, containing modules 5,1/6,1/6,2/7,1/7,2/7,3) is enriched for genes associated with metabolic stress and mitochondrial dysfunction (see Supplementary Table 5, available on the *Arthritis & Rheumatology* web site at http://onlinelibrary.wiley.com/doi/10.1002/art.38679/abstract). Representative modules are shown in Figure 1D. IPA analysis of clusters 1 and 2 is shown in Table 3. Notably, 426 of the 1,098 mitochondrial genes in the mouse MitoCarta database were represented in cluster 2. Of these, 98 (23%) were significantly regulated in the kidneys of mice with disease in late remission after treatment with CTLA-4Ig and TACI-Ig compared with mice with disease in early remission (Figure 2). In addition, of 197 selected genes representing mouse hypoxia, cellular stress and toxicity, and oxidative stress (SABiosciences), 34 were represented in cluster 2 (Figure 2); of these, 8 (23.5%) were significantly regulated in the kidneys of mice with disease in late remission after combination treatment with CTLA-4Ig and TACI-Ig compared with mice with disease in early remission.

Unbiased identification of biomarkers of disease onset, progression, and remission. A second unbiased approach to biomarker identification was to apply an SVD method to the sequential NZB/NZW data sets. This analysis identified genes that were most tightly regulated during changes in disease stage and was performed without consideration of actual fold change in gene expression. Of the top 300 positively and 300 negatively regulated genes within the dominant pattern (see Supplementary Figure 3A, available on the *Arthritis & Rheumatology* web site at http://onlinelibrary.wiley.com/doi/10.1002/art.38679/abstract), 554 with human homologs were differentially expressed between 16-week-old prenephritic mice and 36-week-old mice with proteinuria. These 554 genes were then overlaid on the sets of genes differentially expressed in human SLE biopsy specimens (16,17). Two hundred and one genes were concordantly regulated in the glomeruli and 132 in the tubulointerstitium of human SLE biopsy specimens, with 97 concordantly regulated (31 up-regulated and 66 down-regulated) in both compartments (see Supplementary Table 6A, available on the *Arthritis & Rheumatology* web site at http://onlinelibrary.wiley.com/doi/10.1002/art.38679/abstract). The most highly up-regulated of these 97 genes were associated with myeloid and lymphoid cell infiltration and activation, antigen presentation, and innate immune processes, including ubiquitination, nucleic acid exonuclease activity, and type I IFN

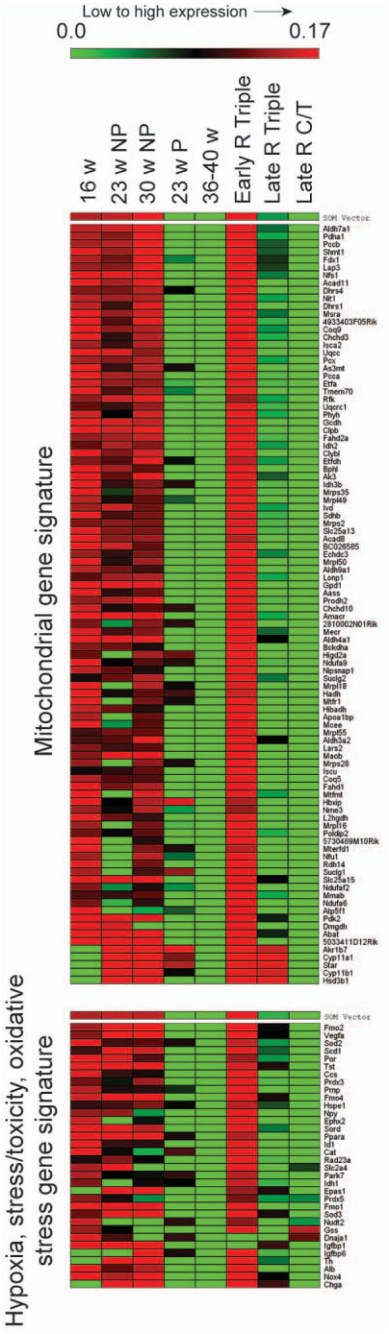

Figure 2. Heatmaps of genes representing the mitochondrial signature (top panel) and the hypoxia, stress/toxicity, and oxidative stress signature (bottom panel) that are present in self-organizing map (SOM) cluster 2 and are regulated in mice during late remission of lupus nephritis. The heatmaps were generated using the SOM module in MultiExperiment Viewer Application (http://www.tm4.org/). The top bar in each panel (SOM vector) represents an average of the gene expression for the corresponding sample. See Figure 1 for other definitions.

production. UBD (FAT10) was the most highly up-regulated nonimmune gene.

Because the genes thus identified were dominated by those associated with established nephritis, we repeated the analysis using only the first 3 groups of the time series (16-week-old mice, 23-week-old mice without proteinuria, and 23-week-old mice with proteinuria) and the 2 remission groups (Supplementary Figure 3B). Of the top 600 genes in the dominant pattern, 121 were concordantly regulated in human glomeruli and 119 in interstitium, with 81 concordantly regulated in both compartments. Of these 81 genes, 40 (30 up-regulated and 10 down-regulated) were within the subset of 603 genes that were regulated >1.5 fold during both disease onset and remission. The most highly up-regulated of these 40 genes in the human biopsy specimens included genes involved in innate immunity, such as IFIH1, CXCL10, and PLAC8 (Onzin), a regulator of proinflammatory responses. Other up-regulated genes include VCAM1; NMI, an IFNγ- and interleukin-2–induced signaling molecule; CKLF, a chemoattractant; FGL2, a prothrombinase induced during inflammation; and SNAI2, a mediator of epithelial-to-mesenchymal transition (Supplementary Table 6B).

Confirmation by real-time PCR. Results from real-time PCR analyses are shown in Supplementary Table 7 and Supplementary Figure 4, available on the *Arthritis & Rheumatology* web site at http://onlinelibrary.wiley.com/doi/10.1002/art.38679/abstract. There was a high level of concordance with those genes shown to be regulated by microarray, but the PCR was more sensitive and therefore detected expression of some genes not detected by microarray analysis. Of 166 genes, only 4 (CCL2, CCL5, CD52, and LY86) were regulated ≥1.5 fold before nephritis onset, reversed with remission induction, became abnormal again during late remission, and were also expressed in both human glomeruli and tubulointerstitium. FCGR, with a similar expression pattern, was up-regulated in human glomeruli (Figure 3A).

A subset of genes displayed a pattern of regulation at proteinuria onset, reversal with complete remission induction, and re-expression during late remission; many of these were associated with macrophage activation. C1qA, ISG20, CTSS, TGFBI (a component of extracellular matrix), and CYBB (NADPH oxidase 2) were robust markers of progression toward relapse and also highly expressed in human biopsy specimens (Figure 3A). In contrast, TNFRSF12, Serpina3g, Fpr2, Clec4e, and Grem1 were highly associated with disease stage in the mouse tissues but were not detected in

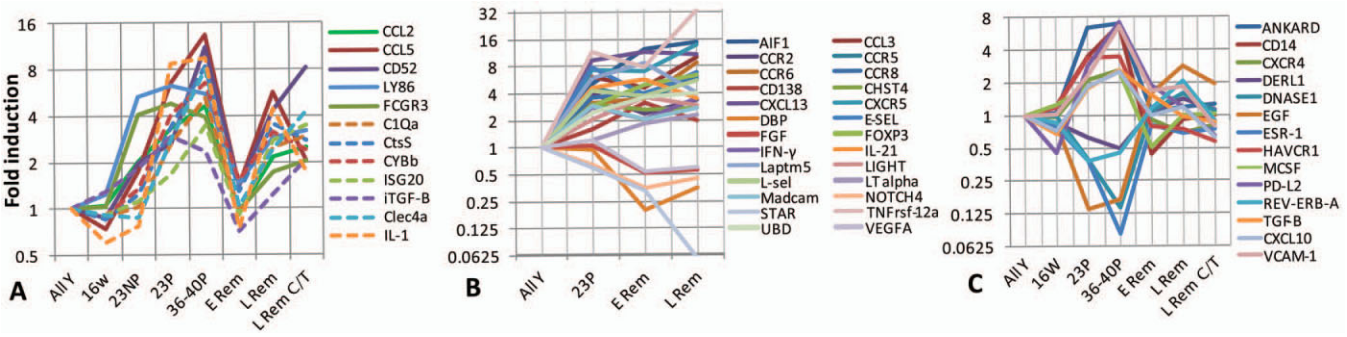

Figure 3. Expression of selected genes in (NZB × NZW)F1 mouse kidneys over time, as determined by polymerase chain reaction. **A,** Genes that were up-regulated prior to proteinuria onset (solid lines) or at proteinuria onset (broken lines), reverted during remission, and became abnormal again during relapse and were also expressed in biopsy specimens from the kidneys of patients with systemic lupus erythematosus. **B,** Genes that were up-regulated at proteinuria onset and did not revert during remission. **C,** Genes that were up-regulated at proteinuria onset, reverted at remission, and remained normal during late remission. All Y = all young mice (pooled data from 6-week-old and 16-week-old mice); E Rem = early remission; L Rem = late remission; L Rem C/T = late remission and treatment with CTLA-4Ig and TACI-Ig. See Figure 1 for other definitions.

human biopsy specimens. Genes that were regulated before proteinuria onset were significantly less likely to revert to normal during remission than genes that were regulated after proteinuria onset ($P = 0.005$) (data not shown).

Up-regulated genes whose expression did not completely revert to normal at remission included a subset of chemokines, cytokines, and adhesion molecules, probably reflecting the incomplete disappearance of lymphoid aggregates, as well as Ubd (FAT10), a marker of tubular epithelial dysfunction. In addition, the down-regulation of VEGFA and FGF2 did not reverse completely with remission induction, suggesting a continuing defect in angiogenesis (Figure 3B).

We confirmed that several genes related to mitochondrial dysfunction or metabolic stress, including NOX4 and COX15, became abnormal late after treatment with CTLA-4Ig/TACI-Ig. In addition, LCN2 and TIMP1, genes that were up-regulated at proteinuria onset and reversed with remission induction, were modestly up-regulated late after treatment with CTLA-4Ig/TACI-Ig before the onset of overt proteinuria.

Finally, we identified a subset of genes whose expression remained at remission levels even during late remission. Up-regulated genes with this pattern included CD14, ANKRD1 (podocyte injury), TGFB, CXCL9, CXCL10, CXCL11, CXCL16, and CCL9 (chemokines), ICAM1 and VCAM1 (endothelial activation), HAVCR1, and C3 (tubular injury), whereas down-regulated genes included EGF, CLYBL, DNASE1, and several genes involved in drug detoxification (Figure 3C).

Application of these data to a second murine model. Of 3,759 genes that were regulated in nephritic versus young NZM2410 mice (17), 2,364 (62.9%) were reversed after BAFF inhibition (see Supplementary Table 8, available on the *Arthritis & Rheumatology* web site at http://onlinelibrary.wiley.com/doi/10.1002/art.38679/abstract), reflecting improvements in inflammation, endothelial cell activation, tubular dysfunction, metabolic stress, and mitochondrial dysfunction. Reversal of nephrin loss suggests that podocyte repair may occur. Of these genes, 399 were concordantly regulated in both the glomeruli and tubulointerstitium of SLE nephritis biopsy specimens; this set of 399 genes was quite similar to that identified in NZB/NZW mice (see Supplementary Table 9, available on the *Arthritis & Rheumatology* web site at http://onlinelibrary.wiley.com/doi/10.1002/art.38679/abstract). After BAFF inhibition, 1,395 genes did not reverse, including both proinflammatory genes and genes related to mitochondrial dysfunction (data not shown), suggesting that, as in NZB/NZW mice, immunomodulation may not completely reverse processes that could contribute to ongoing renal damage.

Quantitative RT-PCR analyses showed increased expression of a subset of proinflammatory cytokines and chemokines in the mice with disease in remission (data not shown), but this was not associated with clinical relapse. As in NZB/NZW mice, a cluster of genes was identified whose expression reversed after remission induction and remained at remission levels even 33 weeks after BAFF-R-Ig therapy (see Supplementary Table 10 and Supplementary Figure 5, available on the

Arthritis & Rheumatology web site at http://onlinelibrary.wiley.com/doi/10.1002/art.38679/abstract).

DISCUSSION

Our study identifies sequential molecular events in the progression and remission of SLE nephritis in informative mouse models. We show limited expression of inflammatory mediators during the prenephritic stage in NZB/NZW mice. In contrast, a major signature of inflammatory cell infiltration and activation occurs at the onset of proteinuria. This is accompanied by increased expression of a variety of collagen genes and evidence of endothelial cell activation, and tubular damage. These changes are associated with glomerular hypertrophy and proliferative changes, and progressive accumulation of periglomerular and perivascular lymphoid aggregates (9).

As glomerular inflammation progresses, compromise of the downstream peritubular blood flow (for review, see ref. 24) is associated with a signature of oxidative and metabolic stress, mitochondrial dysfunction, and tubular damage. In addition, activation of the peritubular endothelium can induce inflammatory cell infiltration, particularly of macrophages, into the tubulointerstitium. We show that disease progression is characterized by continued recruitment of proinflammatory mediators and expression of genes involved in macrophage activation, alternative complement activation, prothrombotic tendency, and fibrosis. Importantly, an unbiased analysis of the sequential microarray data sets from NZB/NZW mice confirms that there are two major gene clusters that are dynamically regulated during disease onset and remission. One, occurring at proteinuria onset, identifies the inflammatory component of nephritis, and the other, occurring during established disease, reflects the metabolic disturbances that are associated with hypoxia.

Previous studies have described the gene expression profiles in NZB/NZW (25) and MRL/*lpr* mouse kidneys (26), including the effect of preventive treatments (rapamycin and prednisone, respectively). Despite the different methods used (e.g., glomeruli laser microdissection in the case of the MRL/*lpr* mouse study), a significant gene overlap (67% and 57%, respectively) was confirmed between our 16-week-old mice versus 36–40-week-old mice data set and the genes that were regulated in mice with established nephritis compared to young mice in those studies.

We further show here that remission induced by costimulatory blockade or BAFF inhibition (9,11) is associated with the reversal of much of the inflammatory signature that accompanies proteinuria onset. Importantly, however, in NZB/NZW mice, the mitochondrial and metabolic signature recurs before the reappearance of proteinuria, perhaps reflecting an increased propensity to hypoxia conferred by the initial tissue insult. In NZM2410 mice, reversal of this signature is incomplete despite histologic remission. In these mice a subset of inflammatory markers and inflammatory cells accumulates during long-lasting remission following BAFF inhibition, but this is not sufficient for clinical relapse. A similar checkpoint has been described in BAFF-deficient NZM2328 mice and in mice congenic for an NZM-derived gene locus that develop glomerular pathology and lymphoid infiltrates but do not progress to renal failure (15,27). These data show that renal decline does not inevitably follow renal inflammatory cell infiltration. Rather, our molecular data suggest that podocyte damage, renal tubular dysfunction, endothelial cell activation, and tissue remodeling are the functional features associated with the clinical onset of proteinuria and consequent renal failure.

Our study gave us an opportunity to identify transcriptional profiles characteristic of each specific disease stage, with the potential to serve as biomarker candidates. Using PCR we identified CCL2, CCL5, LY86, CD52, and FCGR3 as genes that were up-regulated in prenephritic kidneys, fluctuated with early and late remission, and were also highly expressed in human SLE nephritis biopsy specimens. Of these, increasing urinary CCL2 (monocyte chemotactic protein 1) is currently the most promising biomarker for disease flare (28,29), whereas failure to normalize urinary CCL5 (RANTES) during remission is associated with an increased risk of subsequent flare (30). LY86 (MD-1) is expressed by plasma cells and renal macrophages; interestingly, serum levels of soluble LY86 correlate with disease progression in MRL/*lpr* mice (31). CD52 and FCGR3 are markers for infiltrating renal cells. Surprisingly, TNFRSF12 (which encodes for the TWEAK receptor), which is up-regulated in prenephritic mice and is an excellent biomarker for remission and progression, was not detected in our human lupus biopsy specimens. Nevertheless, a previous study using real-time PCR detected TNFRSF12 mRNA in lupus glomeruli and interstitium (32).

Genes that are regulated at proteinuria onset, reverse with remission induction, and become abnormal again during late remission may be useful biomarkers of

impending flare or of failure to respond to therapy. We identified several such genes that are associated with macrophage activation. Of those that were also identified in human kidneys, C1q components are of interest because these are produced mostly by tissue macrophages and may therefore reflect macrophage/DC infiltration and/or activation. Importantly, antibodies to C1q are associated with lupus nephritis, and may amplify tissue damage (33). How C1q modulates local macrophage function in the setting of inflammation is not currently known.

To identify genes whose expression most tightly correlated with disease stage, we used an unbiased approach. Using an NZB/NZW data set that included the prenephritic stage, new-onset proteinuria, and remission, we identified 41 such genes that were also expressed in human SLE biopsy specimens. These include the procoagulant FGL2 and PLAC8 (which encodes onzin), a molecule required for antibacterial and inflammatory responses (34). Two additional genes, CXCL10 and VCAM1, encode soluble proteins that have already been identified as potential urinary biomarkers for human lupus nephritis (5,35,36). In the human biopsy specimens, the expression of CXCL10 was coupled with expression of its inducing protein IFIH1 (MDA5), an IFN-inducible gene that is highly expressed in the glomeruli of SLE nephritis patients (37). Urinary levels of VCAM1 are strongly associated with renal disease activity in mouse and human lupus nephritis in cross-sectional studies (for review, see ref. 35). FGL2 and PLAC8 were regulated at proteinuria onset, reverted with remission induction, and were expressed again during late remission, whereas IFIH1, VCAM1, and CXCL10 remained normal during late remission.

When the whole series of NZB/NZW samples was included in an unbiased analysis of genes regulated with disease stage, 97 genes were identified that were also expressed in both compartments of human SLE biopsy specimens. These included genes involved in innate immunity, many of which are IFN inducible, confirming the sensitivity of genes involved in this pathway to changes in disease activity. Notably, this gene set included LCN2, a marker of proximal tubular damage. While initial longitudinal studies suggested that increasing urine levels of lipocalin 2 (LCN-2) could predict a flare of SLE nephritis, especially in children (38,39), a recent large longitudinal study in adults failed to reproduce these results (40). Our data suggest that LCN-2 is a relatively late marker of SLE nephritis that is highly responsive to remission induction. Indeed, LCN2 was not expressed in the human lupus biopsy specimens, most of which were harvested from patients who had already begun glucocorticoid therapy (17). We also found among this gene set genes whose expression was detected only in mice with proteinuria and remained normal even during late remission. Although such genes may not be sensitive markers of an impending renal flare, they may be of potential use in following up a response to therapy.

Future studies will determine whether the genes we have identified herein can serve as biomarkers for flares or responses to therapy or whether they will help distinguish active disease from chronic changes. While not all of the gene products of our biomarker gene set are soluble, methodology for performing expression, proteomic, or metabolic analysis of urine cells is constantly improving and could be used to test sequential expression of some of the other highly expressed genes or pathways.

Given the current lack of sufficiently effective therapy for lupus nephritis and the unacceptably high rate of disease relapse, one important goal of these studies was to identify pathways and molecules that suggest potential therapeutic targets. While lupus nephritis is classically treated with immunosuppressive therapies, less attention has been paid to the correction of metabolic inefficiency and cellular stress. Multiple strategies to achieve this have been tested in animal models (41,42). In addition, our study has identified several understudied molecules that are tightly regulated with disease stage, highly expressed in the human biopsy specimens, and whose role can be further explored in the appropriate murine models. These include Laptm5, a positive regulator of macrophage proinflammatory cytokine production (43), Plac8 (onzin), and ubiquitin D (FAT10), a proteasome binding protein that promotes tubulointerstitial inflammation in kidney diseases via NF-κB activation (44,45).

In conclusion, our studies show that limited renal chemokine and cytokine production occurs during the prenephritic phase, whereas inflammatory events escalate at or just before proteinuria onset. This is followed by hypoxia and metabolic stress, and finally by tubular and endothelial dysfunction. Regimens that include costimulatory blockade and BAFF inhibition reverse inflammatory events, but progression toward relapse is associated with recurrence of inflammation, cellular stress, and mitochondrial dysfunction. Not all molecular abnormalities are reversed by remission induction therapies, perhaps increasing the sensitivity of the kidney to

hypoxia during flare and contributing to progressive renal damage even during periods of quiescence. In contrast, some molecules maintain their normal expression profile even during the late stages of remission. We show, in sum, that there are several checkpoints along the path to renal failure in lupus nephritis that are associated with renal molecular changes and expression of stage-specific biomarkers, some of which can now be tested in humans.

AUTHOR CONTRIBUTIONS

All authors were involved in drafting the article or revising it critically for important intellectual content, and all authors approved the final version to be published. Dr. Davidson had full access to all of the data in the study and takes responsibility for the integrity of the data and the accuracy of the data analysis.

Study conception and design. Bethunaickan, Berthier, Guan, Kretzler, Davidson.

Acquisition of data. Bethunaickan, Berthier, Guan, Kretzler, Davidson.

Analysis and interpretation of data. Bethunaickan, Berthier, Zhang, Eksi, Li, Guan, Kretzler, Davidson.

REFERENCES

1. Davidson A, Aranow C. Lupus nephritis: lessons from murine models. Nat Rev Rheumatol 2010;6:13–20.
2. Sprangers B, Monahan M, Appel GB. Diagnosis and treatment of lupus nephritis flares—an update. Nat Rev Nephrol 2012;8: 709–17.
3. Costenbader KH, Solomon DH, Winkelmayer W, Brookhart MA. Incidence of end-stage renal disease due to lupus nephritis in the US, 1995–2004 [abstract]. Arthritis Rheum 2008;58 Suppl:S873.
4. Ward MM. Changes in the incidence of endstage renal disease due to lupus nephritis in the United States, 1996–2004. J Rheumatol 2009;36:63–7.
5. Mok CC. Biomarkers for lupus nephritis: a critical appraisal. J Biomed Biotechnol 2010;2010:638413.
6. Li Y, Fang X, Li QZ. Biomarker profiling for lupus nephritis. Genomics Proteomics Bioinformatics 2013;11:158–65.
7. Perry D, Sang A, Yin Y, Zheng YY, Morel L. Murine models of systemic lupus erythematosus. J Biomed Biotechnol 2011;2011: 271694.
8. Theofilopoulos AN, Dixon FJ. Murine models of systemic lupus erythematosus. Adv Immunol 1985;37:269–390.
9. Schiffer L, Sinha J, Wang X, Huang W, von Gersdorff G, Schiffer M, et al. Short term administration of costimulatory blockade and cyclophosphamide induces remission of systemic lupus erythematosus nephritis in NZB/W F1 mice by a mechanism downstream of renal immune complex deposition. J Immunol 2003;171:489–97.
10. Ramanujam M, Wang X, Huang W, Schiffer L, Grimaldi C, Akkerman A, et al. Mechanism of action of transmembrane activator and calcium modulator ligand interactor-Ig in murine systemic lupus erythematosus. J Immunol 2004;173:3524–34.
11. Ramanujam M, Bethunaickan R, Huang W, Tao H, Madaio MP, Davidson A. Selective blockade of BAFF for the prevention and treatment of systemic lupus erythematosus nephritis in NZM2410 mice. Arthritis Rheum 2010;62:1457–68.
12. Schiffer L, Bethunaickan R, Ramanujam M, Huang W, Schiffer M, Tao H, et al. Activated renal macrophages are markers of disease onset and disease remission in lupus nephritis. J Immunol 2008;180:1938–47.
13. Clynes R, Dumitru C, Ravetch JV. Uncoupling of immune complex formation and kidney damage in autoimmune glomerulonephritis. Science 1998;279:1052–4.
14. Bagavant H, Fu SM. New insights from murine lupus: disassociation of autoimmunity and end organ damage and the role of T cells. Curr Opin Rheumatol 2005;17:523–8.
15. Jacob CO, Pricop L, Putterman C, Koss MN, Liu Y, Kollaros M, et al. Paucity of clinical disease despite serological autoimmunity and kidney pathology in lupus-prone New Zealand mixed 2328 mice deficient in BAFF. J Immunol 2006;177:2671–80.
16. Bethunaickan R, Berthier CC, Ramanujam M, Sahu R, Zhang W, Sun Y, et al. A unique hybrid renal mononuclear phagocyte activation phenotype in murine systemic lupus erythematosus nephritis. J Immunol 2011;186:4994–5003.
17. Berthier CC, Bethunaickan R, Gonzalez-Rivera T, Nair V, Ramanujam M, Zhang W, et al. Cross-species transcriptional network analysis defines shared inflammatory responses in murine and human lupus nephritis. J Immunol 2012;189:988–1001.
18. Chan O, Madaio MP, Shlomchik MJ. The roles of B cells in MRL/lpr murine lupus. Ann N Y Acad Sci 1997;815:75–87.
19. Tamayo P, Slonim D, Mesirov J, Zhu Q, Kitareewan S, Dmitrovsky E, et al. Interpreting patterns of gene expression with self-organizing maps: methods and application to hematopoietic differentiation. Proc Natl Acad Sci U S A 1999;96:2907–12.
20. Wall ME, Rechtsteiner A, Rocha L. Singular value decomposition and principal component analysis. In: Berrar DP, Dubitzky W, Granzow M, editors. A practical approach to microarray data analysis. Norwell (MA): Kluwer Academic Publishers; 2003. p. 91–109.
21. Alter O, Brown PO, Botstein D. Generalized singular value decomposition for comparative analysis of genome-scale expression data sets of two different organisms. Proc Natl Acad Sci U S A 2003;100:3351–6.
22. Holter NS, Mitra M, Maritan A, Cieplak M, Banavar JR, Fedoroff NV. Fundamental patterns underlying gene expression profiles: simplicity from complexity. Proc Natl Acad Sci U S A 2000;97: 8409–14.
23. Bethunaickan R, Berthier CC, Zhang W, Kretzler M, Davidson A. Comparative transcriptional profiling of 3 murine models of SLE nephritis reveals both unique and shared regulatory networks. PLoS One 2013;8:e77489.
24. Davidson A, Berthier C, Kretzler M. Pathogenetic mechanisms in lupus nephritis. In: Wallace DJ, Hahn BH, editors. Dubois' Lupus Erythematosus and related syndromes. 8th ed. Philadelphia: Saunders; 2012. p. 237–55.
25. Reddy PS, Legault HM, Sypek JP, Collins MJ, Goad E, Goldman SJ, et al. Mapping similarities in mTOR pathway perturbations in mouse lupus nephritis models and human lupus nephritis. Arthritis Res Ther 2008;10:R127.
26. Teramoto K, Negoro N, Kitamoto K, Iwai T, Iwao H, Okamura M, et al. Microarray analysis of glomerular gene expression in murine lupus nephritis. J Pharmacol Sci 2008;106:56–67.
27. Ge Y, Jiang C, Sung SS, Bagavant H, Dai C, Wang H, et al. Cgnz1 allele confers kidney resistance to damage preventing progression of immune complex-mediated acute lupus glomerulonephritis. J Exp Med 2013;210:2387–401.
28. Brunner HI, Bennett MR, Mina R, Suzuki M, Petri M, Kiani AN, et al. Association of noninvasively measured renal protein biomarkers with histologic features of lupus nephritis. Arthritis Rheum 2012;64:2687–97.
29. Rovin BH, Song H, Birmingham DJ, Hebert LA, Yu CY, Nagaraja HN. Urine chemokines as biomarkers of human systemic lupus erythematosus activity. J Am Soc Nephrol 2005;16:467–73.
30. Tian S, Li J, Wang L, Liu T, Liu H, Cheng G, et al. Urinary levels

of RANTES and M-CSF are predictors of lupus nephritis flare. Inflamm Res 2007;56:304–10.
31. Sasaki S, Nagai Y, Yanagibashi T, Watanabe Y, Ikutani M, Kariyone A, et al. Serum soluble MD-1 levels increase with disease progression in autoimmune prone MRL$^{lpr/lpr}$ mice. Mol Immunol 2012;49:611–20.
32. Michaelson JS, Wisniacki N, Burkly LC, Putterman C. Role of TWEAK in lupus nephritis: a bench-to-bedside review. J Autoimmun 2012;39:130–42.
33. Tsirogianni A, Pipi E, Soufleros K. Relevance of anti-C1q autoantibodies to lupus nephritis. Ann N Y Acad Sci 2009;1173: 243–51.
34. Johnson RM, Kerr MS, Slaven JE. Plac8-dependent and inducible NO synthase-dependent mechanisms clear Chlamydia muridarum infections from the genital tract. J Immunol 2012;188:1896–904.
35. Reyes-Thomas J, Blanco I, Putterman C. Urinary biomarkers in lupus nephritis. Clin Rev Allergy Immunol 2011;40:138–50.
36. Avihingsanon Y, Benjachat T, Tassanarong A, Sodsai P, Kittikovit V, Hirankarn N. Decreased renal expression of vascular endothelial growth factor in lupus nephritis is associated with worse prognosis. Kidney Int 2009;75:1340–8.
37. Imaizumi T, Aizawa-Yashiro T, Tsuruga K, Tanaka H, Matsumiya T, Yoshida H, et al. Melanoma differentiation-associated gene 5 regulates the expression of a chemokine CXCL10 in human mesangial cells: implications for chronic inflammatory renal diseases. Tohoku J Exp Med 2012;228:17–26.
38. Rubinstein T, Pitashny M, Levine B, Schwartz N, Schwartzman J, Weinstein E, et al. Urinary neutrophil gelatinase-associated lipocalin as a novel biomarker for disease activity in lupus nephritis. Rheumatology (Oxford) 2010;49:960–71.
39. Hinze CH, Suzuki M, Klein-Gitelman M, Passo MH, Olson J, Singer NG, et al. Neutrophil gelatinase–associated lipocalin is a predictor of the course of global and renal childhood-onset systemic lupus erythematosus disease activity. Arthritis Rheum 2009;60:2772–81.
40. Kiani AN, Wu T, Fang H, Zhou XJ, Ahn CW, Magder LS, et al. Urinary vascular cell adhesion molecule, but not neutrophil gelatinase-associated lipocalin, is associated with lupus nephritis. J Rheumatol 2012;39:1231–7.
41. Small DM, Coombes JS, Bennett N, Johnson DW, Gobe GC. Oxidative stress, anti-oxidant therapies and chronic kidney disease. Nephrology (Carlton) 2012;17:311–21.
42. Tabas I, Glass CK. Anti-inflammatory therapy in chronic disease: challenges and opportunities. Science 2013;339:166–72.
43. Glowacka WK, Alberts P, Ouchida R, Wang JY, Rotin D. LAPTM5 protein is a positive regulator of proinflammatory signaling pathways in macrophages. J Biol Chem 2012;287: 27691–702.
44. Gong P, Canaan A, Wang B, Leventhal J, Snyder A, Nair V, et al. The ubiquitin-like protein FAT10 mediates NF-κB activation. J Am Soc Nephrol 2010;21:316–26.
45. Ren J, Wang Y, Gao Y, Mehta SB, Lee CG. FAT10 mediates the effect of TNF-α in inducing chromosomal instability. J Cell Sci 2011;124:3665–75.